

# Surface Organometallic Chemistry on Metals: Evidence for the Formation of a Stable $(\text{Rh}_s)_2\text{Ge}(\text{H})(\text{CH}_2)_4\text{OH}$ Fragment at the Surface of a Rhodium Nanoparticle

Emmanuel Tena,<sup>†</sup> Michel Spagnol,<sup>‡</sup> Jean-Pierre Candy,<sup>\*,†</sup> Aimery de Mallmann,<sup>†</sup> Steven Fiddy,<sup>§,||</sup> Judith Corker,<sup>§</sup> and Jean-Marie Basset<sup>†</sup>

LCOMS, UMR CNRS–CPE 9986, 43 bd du 11 novembre 1918, 69616 Villeurbanne, France,  
Rhodia, Centre de Recherche de Lyon, 85 av Frères Perret, 69190 Saint Fons, France,  
Department of Chemistry, The University of Southampton, Highfield,  
Southampton, SO17 1BJ, United Kingdom, and ESRF, 6 rue Jules Horowitz,  
38043, Grenoble Cedex, France

Received December 6, 2002. Revised Manuscript Received January 30, 2003

A grafted organogermanium moiety was observed on a rhodium surface, starting with an organogermane compound,  $(\text{Ad})\text{GeH}_3$  (Ad = adamantyl) (Taoufik et al. *J. Am. Chem. Soc.* **1996**, *118*, 4167). Recently, new surface germanium complexes with functional groups grafted on Pt and Rh particles were prepared by reaction under hydrogen in propan-2-ol of organogermane complexes  $\text{H}_3\text{GeR}^f$  ( $\text{R}^f = -\text{R}-\text{OH}$  or  $\text{R}-\text{OMe}$ ) with the surface of rhodium catalysts (Tena et al. *J. Mol. Catal.* **1999**, *146*, 53). It is proposed that grafted organometallic fragments with formula  $\text{Rh}_s[\text{H}_x\text{GeR}_y^f]_z/\text{SiO}_2$  could be stabilized on the metallic surface. This paper reports the characterization by various physical techniques of the surface complexes obtained by reaction of  $\text{H}_3\text{Ge}-(\text{CH}_3)_4-\text{OH}$  with the reduced surface of rhodium catalysts supported on silica.

## Introduction

Preparation of nanoparticles of known size and composition are more and more important in the field of catalysis, material sciences, microelectronics, optoelectronics, and so forth. To improve their physical and chemical properties, it is of particular importance to be able to cover their surface with appropriate functionalized molecular fragments. We have shown that it was possible to prepare nanoparticles of  $\text{Rh}$ ,<sup>1–3</sup>  $\text{Ni}$ ,<sup>4</sup> or  $\text{Pt}$ <sup>5</sup> covered with  $-\text{SnR}_x$  fragments ( $\text{R} = \text{Me}$ ,  $n\text{-Bu}$ ;  $x = 1, 2, 3$ ). These grafted organometallic fragments, or the species derived from them, are covalently bonded to the particles via one, two, or three covalent bonds which make the surface fragment quite strongly attached to the particle which become quite hydrophobic when the R group is an alkyl or an aryl fragment. This covalent bonding also ensures a stable organization at short or long distance of the chain around the particles. With organogermanium compounds, we demonstrated that

$\text{GeR}_4$  ( $\text{R} = n\text{-Bu}$ ) reacts with silica-supported rhodium particles with formation of organogermanium fragments grafted on the metallic surface.<sup>6</sup> More recently, with use of  $\text{H}_3\text{GeR}$  ( $\text{R} = \text{adamantyl}^1$  or  $\text{R} = -(\text{CH}_2)_3\text{CH}_2\text{OH}^2$ ),  $\text{Rh}_s[\text{Ge}(\text{H})\text{R}_x]_y/\text{SiO}_2$  modified nanoparticles were obtained. The structure of these particles was determined by various physical techniques, but the exact nature of the bond formed between the rhodium surface atoms and the organogermanium moieties was not precisely determined. In this paper, we will use the EXAFS technique in addition to infrared spectroscopy and volumetric measurements to specify the structure of the grafted fragments obtained by reacting  $\text{H}_3\text{Ge}(\text{CH}_2)_3\text{CH}_2-\text{OH}$  with the surface of a rhodium nanoparticle supported on silica.

## Experimental Section

**Materials.** The silica support Aerosil 200 was purchased from Degussa. Its surface area is about  $200 \text{ m}^2 \cdot \text{g}^{-1}$ . Silica-supported rhodium nanoparticles were prepared according to a classical method of exchange and reduction.<sup>7</sup> The rhodium salt,  $\text{RhCl}(\text{NH}_3)_4(\text{OH})_2$ , was purchased from STREM Chem. Inc. The ionic exchange is achieved by stirring the slurry of the silica and the rhodium salt for 10 h at room temperature. After filtration, the surface complex obtained is decomposed by calcination under a mixture of nitrogen/oxygen (5/1) at increasing temperatures from 298 to 673 K ( $1 \text{ K min}^{-1}$ ). The solid obtained is then reduced under flowing hydrogen at 673 K for 4 h and then stored at room temperature in air. The

\* To whom correspondence should be addressed. E-mail: candy@cpe.fr.

<sup>†</sup> UMR CNRS–CPE.

<sup>‡</sup> Centre de Recherche de Lyon.

<sup>§</sup> The University of Southampton.

<sup>||</sup> ESRF.

(1) Taoufik, M.; Santini, C. C.; Candy, J. P.; de Mallmann, A.; Basset, J. M. *J. Am. Chem. Soc.* **1996**, *118*, 4167.

(2) Tena, E.; Candy, J. P.; Cornil, M. F.; Jousseau, B.; Spagnol, M.; Basset, J. M. *J. Mol. Catal.* **1999**, *146*, 53.

(3) Didillon, B.; Houtman, C.; Shay, T.; Candy, J. P.; Basset, J. M. *J. Am. Chem. Soc.* **1993**, *115*, 9380.

(4) Lesage, P.; Clause, O.; Moral, P.; Didillon, B.; Candy, J. P.; Basset, J. M. *J. Catal.* **1995**, *155*, 238.

(5) Humblot, F.; Didillon, B.; Le Peltier, F.; Candy, J. P.; Corker, J.; Clause, O.; Bayard, F.; Basset, J. M. *J. Am. Chem. Soc.* **1998**, *120*, 137.

(6) Didillon, B.; Candy, J. P.; Le Peltier, F.; Ferretti, O. A.; Basset, J. M. *Stud. Surf. Sci. Catal. Heterogen. Catal. Fine Chem. III* **1993**, *78*, 147.

(7) Candy, J. P.; El Mansour, A.; Ferretti, O. A.; Mabilon, G.; Bournonville, J. P.; Basset, J. M.; Martino, G. *J. Catal.* **1988**, *112*, 201.

starting organogermane compound  $\text{H}_3\text{Ge}-(\text{CH}_3)_4-\text{OH}$  (**1**) was prepared according to the procedure already described.<sup>2</sup> The infrared spectra of pure **1** is reported in Figure 2a.

**Electron Microscopy (CTEM).** Conventional transmission electron microscopy (CTEM) was performed using a JEOL 100 CX electron microscope to establish particle size distributions.

**Chemisorption Measurements.** Gas adsorption measurements were carried out at room temperature using conventional Pyrex volumetric adsorption equipment.<sup>8</sup> The catalyst sample was placed in a Pyrex flow-through cell to enable reduction in flowing hydrogen at 723 K. After reduction, the cell was sealed and the sample was outgassed at 723 K for 2 h under vacuum before gas chemisorption measurements. The vacuum ( $10^{-6}$  mbar) was achieved with a liquid-nitrogen-trapped mercury diffusion pump. The equilibrium pressure was measured with a Texas Instrument gauge (pressure range 0–1000 mbar with an accuracy of 0.1 mbar).

**Extended X-ray Adsorption Fine Structure (EXAFS).** X-ray absorption spectra were recorded on the station DCI at the LURE synchrotron radiation facility (operating at 1.85 GeV with an average current of ca. 300 mA) using a Si(311) double-crystal monochromator and two Ar-filled ionization chambers as detectors. Powdered samples for EXAFS analysis were prepared as described above under the strict exclusion of air. EXAFS cells (ca 0.5–1.0-cm thick) fitted with Kapton windows were built onto break-seal Pyrex tubes containing the silica-supported samples and evacuated to ca. 0.01 Pa before sample transfer under argon. X-ray absorption spectra were acquired in the transmission mode at room temperature at the Ge K edge (11103 eV), from 10900 to 11900 eV by 2-eV steps with a counting time of 1.0 s/point. In these conditions an absorption edge  $\Delta\mu$  of ca. 0.2 was observed. The spectrum of the sample (0.51 Ge wt %) resulted from the average of seven such recordings. Background-subtracted EXAFS data were obtained using software written by Michalowicz.<sup>9</sup> Spherical wave curve fitting analysis was carried out using ab initio phase shifts and backscattering amplitudes calculated by FEFF 7.<sup>10</sup> A solution of  $\text{GeBu}_4$  in heptane was used as a reference and the simulation of the spectrum was very satisfactory using the theoretical phase shifts and backscattering amplitudes thus generated (first shell: 4 C at 0.1966 nm;  $2\sigma^2 = 0.0055$ ). The accuracy of bonded and nonbonded interatomic distances is considered to be 1.4% and 1.6%, respectively.<sup>11,12</sup> Precisions on the first shell coordination numbers are estimated to be ca. 5–10% and between 10 and 20% for nonbonded shells. The  $\rho$ -factor is defined as  $(\sum[k^3\chi^T - k^3\chi^E]^2 / \sum[k^3\chi^E]^2) \times 100\%$  where  $\chi^T$  and  $\chi^E$  are the theoretical and experimental normalized oscillatory parts of the absorption coefficient and  $k$  is the intensity of the photoelectron wave vector.

**Hydrogenolysis of  $\text{H}_3\text{Ge}(\text{CH}_2)_4\text{OH}$  on Silica Support and on Reduced Rh Particles.** This reaction was performed in the same apparatus as for chemisorption measurements following the procedure already described for  $\text{Sn}(n\text{-C}_4\text{H}_9)_4$  reaction with silica-supported rhodium.<sup>3</sup> After reduction under flowing  $\text{H}_2$ , the sample (silica or silica-supported rhodium) was sealed under  $\text{H}_2$  and then kept at room temperature under 30 mbar of  $\text{H}_2$ . The desired amount of  $\text{H}_3\text{Ge}(\text{CH}_2)_4\text{OH}$  was then carefully introduced into the reactor via a septum to avoid contact with air. The reaction was performed at 323 K. The gases evolved during the reaction were trapped at 77 K (liquid-nitrogen temperature) elsewhere in the apparatus, to avoid possible feedback of the gases onto the catalytic surface and further hydrogenolysis. The total pressure in the reactor was continuously measured to obtain a precise measurement of the

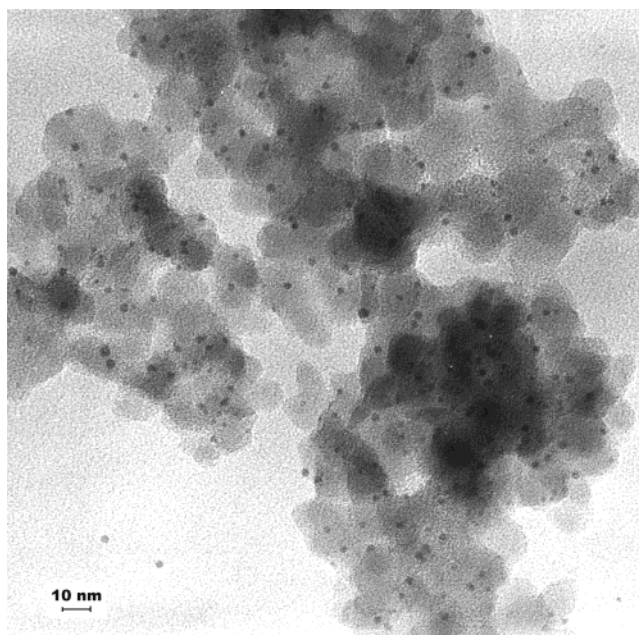


**Figure 1.** TEM picture of Rh particles on silica.

amount of gas untrapped at 77 K. After various times of reaction, the reactor was isolated and the temperature of the cold part was raised to room temperature. The gases evolved were qualitatively and quantitatively analyzed by GC and volumetric measurements. The trap was then cooled with liquid nitrogen and reconnected to the reactor and the reaction pursued. At the end of the reaction, the gas phase is evacuated and about 30 mbar of CO is introduced into the reactor. The remaining chemisorbed hydrogen is then displaced by CO and it can be analyzed by GC. After that, the solid was washed with propanol and the amount of unreacted  $\text{H}_3\text{Ge}(\text{CH}_2)_3\text{CH}_2\text{OH}$  was measured by GC. The sample was then dried in an oven at 360 K and the amount of germanium grafted was determined by elemental analysis.

**Infrared Spectroscopy.** The infrared spectrometer is a FTIR apparatus Nicolet 550. The reaction between  $\text{H}_3\text{Ge}(\text{CH}_2)_4\text{OH}$  and  $\text{Rh}/\text{SiO}_2$  was performed in sealed tube reactors pre-equipped with break-seal tubes for the introduction of nongaseous reactants and  $\text{CaF}_2$  windows to allow acquisition of infrared spectra, as described elsewhere.<sup>13</sup>

## Results and Discussion

The metal loading of the  $\text{Rh}/\text{SiO}_2$  solid, determined by elemental analysis, is 1.19% (w/w). The particle size distribution determined by CTEM analysis is narrow with an average particle diameter of 1.2 nm. According to CTEM (Figure 1), the particles present a spherical shape; the dispersion of the metallic particles, which is the number of surface Rh atoms per total number of Rh atoms ( $D = \text{Rh}_s/\text{Rh}$ ), is ca. 0.8. The dispersion of the metallic particles, measured by hydrogen chemisorption, assuming the stoichiometries of 1.3  $\text{H}/\text{Rh}_s$  at 300 K for an equilibrium pressure of 150 mbar<sup>7</sup> is close to 0.8.

When  $\text{H}_3\text{Ge}(\text{CH}_2)_3\text{CH}_2\text{OH}$  (0.077 mmol) **1** is contacted, without solvent, at 300 K with 1 g of  $\text{Rh}/\text{SiO}_2$  ( $\text{Ge}/\text{Rh}_s = 0.82$ ), there is a fast evolution of hydrogen and of a small amount of propane. After 30 h, the totality of **1** has reacted as there is no traces of **1** extracted by washing the sample with propan-2-ol. The elemental analysis of the sample gives  $\text{Ge}/\text{Rh}_s = 0.72$ .

(8) Candy, J. P.; Fouilloux, P.; Renouprez, A. J. *J. Chem. Soc., Faraday I* **1980**, *76*, 616.

(9) Michalowicz, A. *Logiciel pour la chimie*, Société Française de Chimie: Paris 1991; p 102.

(10) Zabinsky, S. I.; Rehr, J. J.; Ankudinov, A.; Albers, R. C.; Eller, M. J. *Phys. Rev. B: Condens. Matter Mater. Phys.* **1995**, *52*, 2995.

(11) Corker, J.; Evans, J.; Leach, H.; Levanson, W. *J. Chem. Soc., Chem. Commun.* **1989**, 181.

(12) Corker, J.; Evans, J. *J. Chem. Soc., Chem. Commun.* **1994**, 1027.

(13) Quignard, F.; Lecuyer, C.; Bougault, C.; Lefebvre, F.; Choplin, A.; Olivier, D.; Basset, J. M. *Inorg. Chem.* **1992**, *31*, 928.



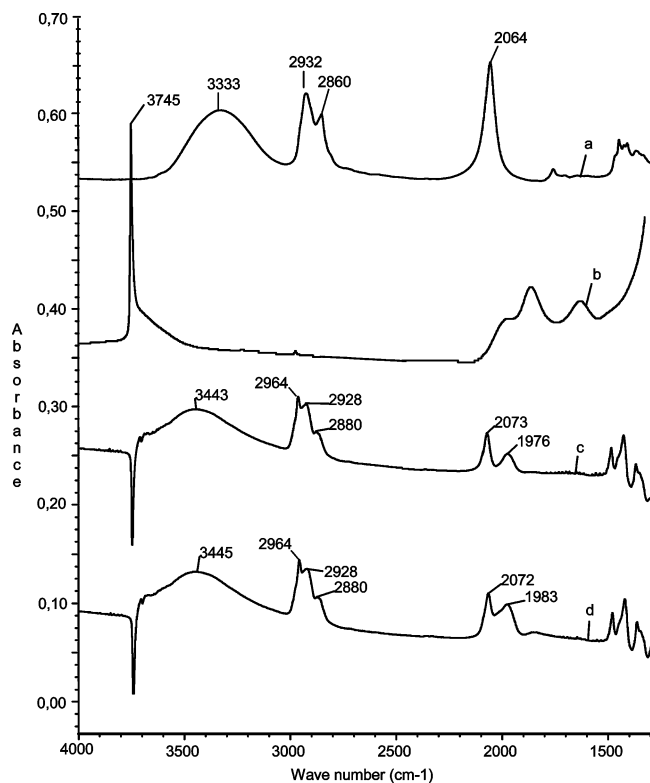


**Figure 2.** Infrared spectra of (a) pure  $\text{H}_3\text{Ge}(\text{CH}_2)_4\text{OH}$ ; (b) 30 mg of  $\text{Rh}/\text{SiO}_2$  reduced at  $400^\circ\text{C}$  under hydrogen and evacuated under vacuum. Spectra (c) correspond to (b) +  $10\ \mu\text{mol}$  of  $\text{H}_3\text{Ge}(\text{CH}_2)_4\text{OH}$  1 h at 298 K and 20 h under vacuum at 298 K and subtraction of reference (b). Spectra (d) correspond to (c) + 10 mbar CO.

This value is not far from the expected value (0.82) if the totality of **1** has reacted and falls into analytical error. The total amount of hydrogen evolved corresponds to  $0.98\ \text{H}_2/\text{Ge}$  and the total amount of propane evolved ( $\text{C}_3\text{H}_8/\text{Ge} = 0.15$ ) suggests the occurrence of a secondary reaction of decarbonylation of the butanol moiety. Adsorption of **1** on dehydroxylated silica is a fully reversible process: When 0.1 mmol of  $\text{H}_3\text{Ge}(\text{CH}_2)_3\text{CH}_2\text{OH}$ , **1**, are reacted with 1 g of dehydroxylated silica, there is no gas evolution, even after 50 h of reaction at 323 K, and the amount of  $\text{H}_3\text{Ge}(\text{CH}_2)_3\text{CH}_2\text{OH}$  which can be extracted intact by washing with propan-2-ol at the end of the interaction is about 99%. These data are in agreement with the formation on the rhodium surface of the hypothetical surface compound  $\text{Rh}_s[\text{Ge}(\text{H})\text{R}^{f_{0.85}}]_{0.8}$ .

Infrared spectroscopy of pure **1** in the range  $4000\text{--}1300\ \text{cm}^{-1}$  is reported in Figure 2a. The band at  $3333\ \text{cm}^{-1}$  is attributed to the  $\nu(\text{O-H})$  vibration of the alcohol group, the band at  $2064\ \text{cm}^{-1}$  is attributed to the  $\nu(\text{Ge-H})$  vibration, and the bands at  $2932$  and  $2860\ \text{cm}^{-1}$  are attributed to the  $\nu(\text{C-H})$  vibrations of the  $\text{CH}_2$  groups.

Whereas, after absorption of **1** on pure silica, the treatment of the sample under vacuum for 30 h leads to complete disappearance of the bands attributed to the ligands, on  $\text{Rh}/\text{SiO}_2$  the bands at  $2928$  and  $2880\ \text{cm}^{-1}$  (attributed to the  $\nu(\text{C-H})$  vibrations of the  $\text{CH}_2$  groups),  $2964\ \text{cm}^{-1}$  (assigned to the  $\nu(\text{C-H})$  vibrations of the  $\text{CH}_3$  group), and  $2073\ \text{cm}^{-1}$  (attributed to the  $\nu(\text{Ge-H})$  vibration) remained after a vacuum treatment (Figure 2c). The band characteristic of the free silanol groups<sup>14</sup> at  $3745\ \text{cm}^{-1}$  decreases after adsorption of **1** and vacuum treatment. It is suggested that some of the

silanol groups interact with the OH groups of the ligand. It was demonstrated<sup>15,16</sup> that the interaction of the silanol groups with adsorbed  $\text{H}_2\text{O}$  results in a low-frequency shift of the  $\nu(\text{O-H})$  vibration of the silanol group from  $3745$  to  $3520\ \text{cm}^{-1}$ . It is difficult to discriminate between the  $\nu(\text{O-H})$  vibration of the alcohol group ( $3333\ \text{cm}^{-1}$ ) and of the bonded silanol group ( $3520\ \text{cm}^{-1}$ ); therefore, the broad band at  $3443\ \text{cm}^{-1}$  must be a superposition of the two  $\nu(\text{O-H})$  vibrations. The chemisorption process has preserved an "hydrido" ligand ( $\text{Ge-H}$ ), the  $\text{CH}_2$  fragments as well as the OH functionality. A small band was observed at  $1976\ \text{cm}^{-1}$  (Figure 2c). When CO (10 mbar) is introduced (Figure 2d) on the sample, there is a slight, but clear, increase of the intensity of this band with a slight increase of its frequency ( $1983\ \text{cm}^{-1}$ ). It is suggested that the band at  $1976\ \text{cm}^{-1}$  observed after 20 h of reaction is due to a very small amount of adsorbed CO. This band appeared concomitantly with the  $2964\text{-cm}^{-1}$  band, associated with  $\text{CH}_3$  groups. It seems that a small amount of the  $-(\text{CH}_2)_4\text{OH}$  groups is decarbonylated into  $-(\text{CH}_2)_2\text{CH}_3$ , CO, and  $\text{H}_2$ . The presence of a carbonyl band  $\nu(\text{CO})$  at  $1976\ \text{cm}^{-1}$ , corresponding to a small amount of CO (note that carbonyls have a very high extinction coefficient), is in agreement with the detection of traces of propane. The  $\nu(\text{CO})$  band of the CO linearly coordinated on a reduced rhodium surface is generally observed at  $2059\ \text{cm}^{-1}$  at full coverage and at lower frequencies at low coverage or on a tin-modified surface.<sup>3</sup> The shift of this band could be due to both the electronic effect of the organometallic fragment in close vicinity to the adsorbed CO and the geometric effect coming from the decrease of CO coverage.<sup>3,17,18</sup> From volumetric measurement, the amount of CO adsorbed on the  $\text{Rh}_s[\text{Ge}(\text{H})\text{R}^{f_{0.85}}]_{0.8}$  sample is estimated to be ca.  $0.2\ \text{CO}/\text{Rh}_s$ . As the surface coverage of the rhodium particle by the organometallic fragment is lower than 1 (about 0.8), it is proposed that the adsorbed CO is located on the "free" surface rhodium atoms.

EXAFS was applied to detect the "hypothetical", but "expected", presence of  $\text{Rh-Ge}$  (or  $\text{Rh=Ge}$ )<sup>1</sup> and  $\text{Ge-C}$  bonds (suggesting covalent attachment to the rhodium surface) for the grafted organometallic fragment  $\text{Rh}_s[\text{Ge}(\text{H})\text{R}^{f_{0.85}}]_{0.8}$ . The best fit to the  $k^3$ -weighted EXAFS data of the sample is shown in Figure 3 with a model comprising 1.4 carbon at  $0.187\ \text{nm}$  and 1.8 rhodium at  $0.245\ \text{nm}$  (Table 1).

The EXAFS-derived distance for the  $\text{Ge-C}$  bond ( $0.187\ \text{nm}$ ) is shorter than the bond length expected for a  $\text{Ge-C}$   $\sigma$  bond ( $0.193\ \text{nm}$ ;<sup>19</sup>  $0.195\ \text{nm}$ <sup>20</sup> or  $0.196\ \text{nm}$  in  $\text{GeBu}_4$ , our reference compound). The shortening of the bond may suggest the possible presence of some  $\text{Ge-O}$  bond contribution ( $\text{Ge-O}$   $\sigma$  bond  $0.170\ \text{nm}$ ;<sup>21</sup>  $0.177\ \text{nm}$ <sup>22</sup>). To try and elucidate the presence of  $\text{Ge-O}_{\text{surface}}$

(14) Nédez, C.; Théolier, A.; Lefebvre, F.; Choplin, A.; Basset, J. M.; Joly, J. F. *J. Am. Chem. Soc.* **1993**, *115*, 722.

(15) Sheppard, N. *Spectrochim. Acta* **1959**, *14*, 249.

(16) Muster, T. H.; Prestidge, C. A.; Hayes, R. A. *Colloids Surf.* **A** **2001**, *176*, 253.

(17) Humblot, F.; Candy, J. P.; Le Peltier, F.; Didillon, B.; Basset, J. M. *J. Catal.* **1998**, *179*, 459.

(18) Sachtler, W. M. H.; Van Santen, R. A. *Adv. Catal.* **1977**, *26*, 69.

(19) Gurkova, S. N.; Gusev, A. I.; Alexeev, N. V.; Gar, T. K.; Viktorov, N. A. *Zh. Strukt. Khim.* **1985**, *26*, 148.

(20) Ferguson, G.; Glidewell, C. *Acta Crystallogr., Sect. C: Cryst. Struct. Commun.* **1996**, 1889.

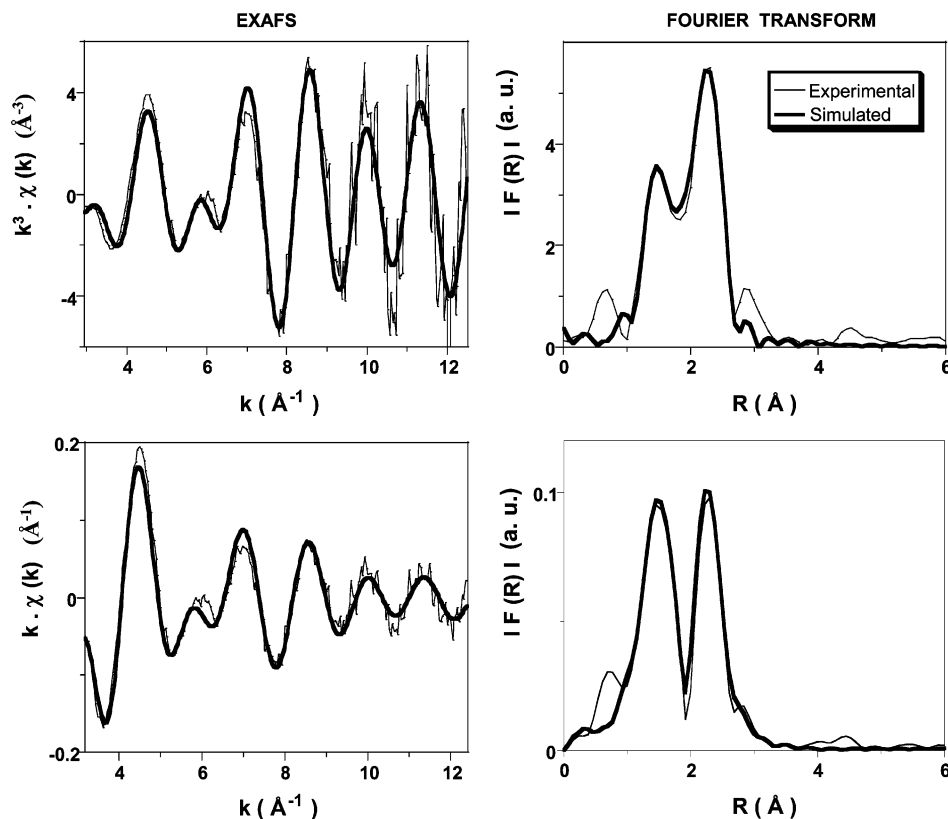


**Figure 3.** Ge K-edge  $k^1$ - and  $k^3$ -weighted EXAFS (left) and Fourier transform ( $R$  values not corrected from phase shifts) (right) of RhGe(H)R'/SiO<sub>2</sub> species formed at 25 °C under vacuum; experimental (thin line) and spherical wave theory (bold line).

**Table 1. Ge K-Edge EXAFS Derived Structural Parameters for RhGe(H)R'/SiO<sub>2</sub> Species Formed at 25 °C under Vacuum<sup>a</sup>**

shell	coordination no.	distance (nm)	$\rho$ -factor (%)	$2\sigma^2$ (Å <sup>2</sup> )
C	$1.4 \pm 0.2$	$0.187 \pm 0.001$	14	0.0028
Rh	$1.8 \pm 0.2$	$0.245 \pm 0.001$		0.0125

<sup>a</sup> For Ge K-edge spectra;  $\Delta E$  value for this sample is 3.0 eV;  $\sigma$ , Debye–Waller factor.

bonding, analysis of the light scatter was first conducted using  $k^3$ -weighted EXAFS and then by using  $k^1$ -weighted EXAFS to try and emphasize the scattering produced by the light backscatters at low  $k$ . The best model to the  $k^1$ -weighted data was found to be 1.4 C at 0.186 nm and 1.8 Rh at 0.245 nm (Figure 3), matching with high accuracy the model used to fit the  $k^3$ -weighted data. The addition of extra Ge–O bonds and/or the replacement of one of the carbons by an oxygen only resulted in higher  $\rho$ -factors and/or significant differences in the backscattering phases between the experimental and the theoretical data. The presence of a small amount of germanium species linked to oxygen atoms of the silica surface cannot be completely excluded since it could explain the high value found for the number of light atoms in the first shell ( $1.4 \pm 0.2$  instead of 1 expected) and the low value found for the number of heavy atoms ( $1.8 \pm 0.2$  instead of 2 expected). However, the inclusion of a third shell of ca. 0.4 Si at 0.334 nm gave a very slight improvement in the fit but this shell was not considered statistically significant. The germa-

nium–rhodium distance (0.245 nm) falls within the range of singly bound Ge–M previously reported in the literature (Ge–Ru (0.248 nm),<sup>23</sup> Ge–Ir (0.248 nm),<sup>24</sup> Ge–Ru (0.240 nm),<sup>25</sup> Ge–Co (0.247 nm),<sup>26</sup> Ge–Pt (0.243 nm)<sup>27</sup>); typically, Ge–M distances are observed between 0.24 and 0.248 nm, whereas Ge=M distances, as observed for germylene species, are typically 0.012–0.017 nm shorter<sup>28</sup> and will therefore fall within the range 0.223–0.236 nm. The fitting of a Ge=Rh distance between 0.225 and 0.235 nm only gave worse  $\rho$ -factors and a very poor fit of the model to the experimental magnitude function, suggesting that this type of species is not present. This provides good evidence for the presence of *singly bound* Ge species to the rhodium surface.

Attempts to try and fit Ge–Ge bonds only resulted in either negative/very low Debye–Waller factors or a higher  $\rho$ -factor and a considerably worse fit. The presence of either rhodium or germanium nearest neighbors was clarified further by the examination of the sine/modulus functions of the Rh and Ge shells. It was found that, again in this situation, the rhodium backscattering phases matched the experimental phases much better than the germanium phases, especially at high  $k$  values.<sup>28</sup>

(23) Ball, R.; Bennett, M. J. *Inorg. Chem.* **1972**, *11*, 1806.

(24) Bell, N. A.; Glockling, F.; Schneider, M. L.; Shearer, H. M. M.; Wilbey, M. D. *Acta Crystallogr., Sect. C: Cryst. Struct. Commun.* **1984**, *40*, 625.

(25) Chan, L. Y. Y.; Graham, W. A. G. *Inorg. Chem.* **1975**, *14*, 1778.

(26) McIndoe, J. S.; Nicholson, B. K. *J. Organomet. Chem.* **1999**, *577*, 181.

(27) Yamashita, H.; Kobayashi, T.; Tanaka, M.; Samuels, J. A.; Streib, W. E. *Organometallics* **1992**, *11*, 2330.

(28) Litz, K. E.; Henderson, K.; Gourley, R. W.; Holl, M. M. B. *Organometallics* **1995**, *14*, 5008.

(21) Morosin, B.; Harrah, L. A. *Acta Crystallogr., Sect. B: Struct. Sci.* **1981**, *59*.

(22) Bravo-Zhivotovskii, D.; Apeloig, Y.; Ovchinnikov, Y.; Igonin, V.; Struchkov, Y. T. *J. Organomet. Chem.* **1993**, *123*.

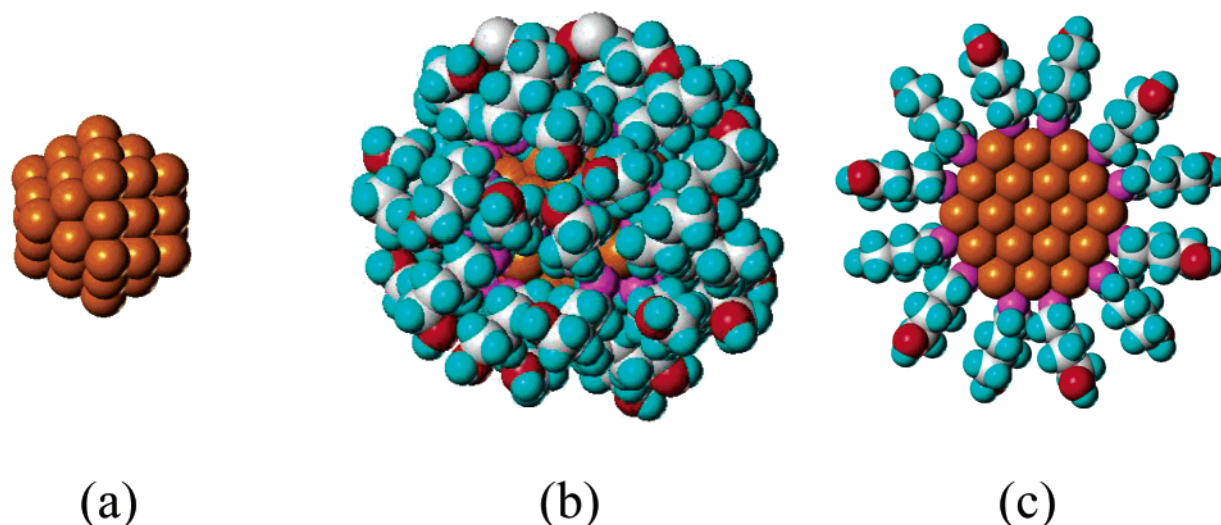


**Figure 4.** (a) Ideal rhodium particle, (b) rhodium particle modified by surface organogermeryl fragments ( $\mu_2$ -Ge(H)(CH<sub>2</sub>)<sub>3</sub>CH<sub>2</sub>OH) after reaction with H<sub>3</sub>Ge(CH<sub>2</sub>)<sub>3</sub>CH<sub>2</sub>OH (Ge/Rh<sub>s</sub> = 1), and (c) cross section of (b).

Figure 4 represents a pure rhodium particle and the cross section of a rhodium particle covered with the surface organogermeryl fragment ( $\mu_2$ -Ge(H)(CH<sub>2</sub>)<sub>3</sub>CH<sub>2</sub>OH) after reaction with H<sub>3</sub>Ge(CH<sub>2</sub>)<sub>3</sub>CH<sub>2</sub>OH. This representation is obtained using "Sybyl" Molecular Modelisation software from "Tripos Associates"<sup>29</sup> running on an "O<sub>2</sub>" computer from Silicon Graphics. We used the Tripos force field, 0.245 nm for the Rh–Ge distance, and 0.187 nm for the Ge–C distance. It can be observed that there is no steric hindrance for the full coverage of the rhodium particle with the organometallic fragments.

### Conclusions

H<sub>3</sub>GeR<sup>f</sup> with R<sup>f</sup> = (CH<sub>2</sub>)<sub>3</sub>CH<sub>2</sub>OH reacts selectively at 300 K on the reduced surface of silica-supported rho-

dium particles to form the Rh<sub>s</sub>[Ge(H)R<sup>f</sup><sub>0.85</sub>]<sub>0.8</sub> surface complex. The >Ge(H)R<sup>f</sup><sub>0.85</sub> fragment is grafted on two adjacent surface rhodium atoms by two single Rh–Ge bonds. Some of the R<sup>f</sup> groups are in interaction with the silanol groups of the silica surface. The hydrogenolysis of a part of the Ge–R<sup>f</sup> bond (about 10%) and the decarbonylation of R<sup>f</sup>, –CH<sub>2</sub>(CH<sub>2</sub>)<sub>2</sub>CH<sub>2</sub>OH, to form the >Ge(H)C<sub>3</sub>H<sub>7</sub> fragment and adsorbed CO (or propane and adsorbed CO) are also observed. The presence of few ≡Ge–R<sup>f</sup> fragments grafted on the silica surface may also be proposed, based on the EXAFS observation.

**Acknowledgment.** The authors greatly thank the L.U.R.E. (Orsay, France), Valérie Briois, and Stéphanie Belin for EXAFS facilities. Molecular Modelisation was done by François Bayard from LCOMS-CPE (Villeurbanne, France).

(29) Tripos. Tripos Associates, 1699 S. Hanley Road, Suite 303, St. Louis, MO 63144.